HHS Public Access

Author manuscript

Nat Immunol. Author manuscript; available in PMC 2015 November 01.

Published in final edited form as:

Nat Immunol. 2015 May ; 16(5): 458–466. doi:10.1038/ni.3130.

Jnk2 promotes stress-induced mitophagy and suppresses inflammasome activation by targeting smARF for degradation

Qiao Zhang[1,2,5], **Hong Kuang**[1,2,5], **Cong Chen**[1], **Jie Yan**[3], **Hanh Chi Do-Umehara**[1], **Xin-yuan Liu**[2], **Laura Dada**[1], **Karen M. Ridge**[1,4], **Navdeep S. Chandel**[1], and **Jing Liu**[1]

[1]Division of Pulmonary and Critical Care Medicine, Feinberg School of Medicine, Northwestern University, Chicago, IL 60611, USA

[2]State Xinyuan Institute of Medicine and Biotechnology, College of Life Science, Zhejiang Sci-Tech University, Hangzhou 310018, China

[3]Ben May Department for Cancer Research, The University of Chicago, Chicago, IL 60637

[4]Jesse Brown Veterans Affairs Medical Center, Chicago, IL 60612, USA

Abstract

Mitophagy is essential for cellular homeostasis but the regulatory mechanism is largely unknown. Here we report that the kinase Jnk2 is required for stress-induced mitophagy. Jnk2 promoted ubiquitination and proteasomal degradation of small mitochondrial form of ARF (smARF). Loss of Jnk2 led to accumulation of smARF, which in turn induced excessive autophagic activity, resulting in lysosomal degradation of the mitophagy adaptor p62 in the steady state. The depletion of p62 prevented Jnk2-deficient cells from mounting mitophagy upon stress. Jnk2-deficient mice displayed defective mitophagy, resulting in tissue damage under hypoxic stress, as well as hyperactivation of inflammasome and increased mortality in sepsis. Our finding defines a unique mechanism of maintaining immune homeostasis that protects the host from tissue damage and mortality.

INTRODUCTION

Mitophagy, a selective form of autophagy that removes damaged or excessive mitochondria, is essential in maintaining cellular energy homeostasis and functions[1,2]. Deregulation of mitophagy has been implicated in many pathophysiological activities and diseases[1,2]. Accumulating evidence suggests that mitophagy plays a crucial role in the regulation of immune responses[3–5]. Defects in clearance of damaged mitochondria by mitophagy result in the production of excessive reactive oxygen species (ROS) and damage-associated molecular patterns, leading to hyperactivation of NOD-like receptor family, pyrin domain

Correspondence should be addressed to J.L. (jing@northwestern.edu).

[5]These authors contributed equally to this work

AUTHOR CONTRIBUTIONS

Q.Z. and H.K. did experiments and analyzed the data; J.Y, C.C. and H.C.D. did experiments; X.L., L.D., K.M.R. and N.S.C provided reagents; J.L. designed and supervised the study, did experiments, analyzed the data and wrote the manuscript.

containing 3 (NLRP3) inflammasome, which can induce tissue and organ damage and increased mortality in the host[3–5].

The mitophagy machinery has been extensively investigated recently but the detailed mechanism is still largely unclear. A prominent theme is that the E3 ubiquitin ligase Parkin and the PTEN-induced putative kinase 1 (PINK1) mediate the priming of damaged mitochondria for mitophagy[6–9]. PINK1 is constitutively degraded in healthy mitochondria but stabilized on the outer membrane of damaged mitochondria, where it recruits and activates Parkin by phosphorylating Parkin at Ser65 (refs. 6–9). Activated Parkin ubiquitinates mitochondrial substrates, which in turn trigger the translocation of the Ub- and LC3-binding adaptor protein p62 (also known as SQSTM1 or sequestosome-1) or a related protein NBR1 to damaged mitochondria for subsequent formation of autophagosome that will fuse with lysosome (autolysosome) for degradation[1,2,6,8,10–16]. The adaptor protein p62 itself is degraded together with enveloped cytosolic contents in the autolysosome during autophagy and mitophagy, serving as a marker of autophagy, but its abundance is restored at later phase of autophagy/mitophagy through transcriptional upregulation[17,18].

Small mitochondrial ARF (smARF) is a short isoform of the tumor suppressor ARF produced by alternatively translational initiation at Met45 and localizes exclusively to mitochondria[19,20]. The amount of smARF at steady-state conditions is extremely low due to constant degradation by the proteasome[19–21]. Using ectopic expression approaches, it has been reported that overexpression of smARF is capable of inducing mitochondria depolarization and subsequent autophagy and mitophagy[19,20,22]. However, the pathophysiological function and regulation of endogenous smARF is not known.

c-Jun N-terminal protein kinase (Jnk) (also known as stress-activated protein kinase [SAPK])[23] is a subfamily of the mitogen-activated protein kinase (MAPK) superfamily. Jnk is involved in regulation of many cellular activities from gene expression to apoptosis[23–25]. Jnk has two ubiquitously expressed isoforms, Jnk1 and Jnk2, which share 83% amino acid identity with shared and distinct functions[23–25]. It has been shown that Jnk1 is the main Jnk isoform that is activated by a variety of extracellular stimuli, whereas Jnk2 activity is negligible[26]. Instead, in unstimulated cells, Jnk2 targets its substrates for proteasomal degradation, including c-Jun, ATF-2 and p53, independently of its kinase activity[27–31]. Recently, it was reported that Jnk1, but not Jnk2, contributes to starvation-induced autophagy by phosphorylating Bcl-2, leading to its dissociation with Beclin 1 (ref.32). However, it is not known whether these two Jnk isoforms regulate mitophagy. Here we report that Jnk2 promotes ubiquitination-dependent proteasomal degradation of endogenous smARF, which otherwise triggers lysosomal degradation of p62 through augmentation of the steady-state autophagy activity. Jnk2-deficient mice display defective mitophagy, resulting in tissue damage under hypoxic stress, and hyperactivation of inflammasome and increased mortality in sepsis.

RESULTS

Jnk2 is required for stress-induced mitophagy

To understand the role of Jnk in regulation of stress-induced mitophagy, we used Jnk1- or Jnk2-deficient mouse embryonic fibroblasts (MEFs). Immunoblotting analysis showed that mitochondrial proteins (Tom20 for outer membrane, TIM23 and/or ATP5β for inner membrane, and cytochrome C and/or HSP60 for mitochondrial matrix) were significantly reduced in wild-type fibroblasts cultured under hypoxic conditions or treated with CCCP (Carbonyl cyanide m-chlorophenyl hydrazone), or HBSS (Hank's Balanced Salt Solution), compared to cells cultured in normal growth medium (Fig. 1a, b and Supplementary Fig. 1a), consistent with previous reports[33–36]. The reduction was caused by mitophagy, as it was prevented by bafilomycin A1, a lysosomal ATPase inhibitor (Supplementary Fig. 1b, c). Under the same conditions, the reduction of mitochondrial proteins was inhibited in *Jnk2*$^{-/-}$ but not *Jnk1*$^{-/-}$ MEFs (Fig. 1a, b and Supplementary Fig. 1d–g). The ratio of green fluorescent protein (GFP)-LC3 punctation that localized with mitochondria was significantly lower in *Jnk2*$^{-/-}$ MEFs when compared to wild-type fibroblasts (Fig. 1c, d). Defects in mitochondrial clearance in *Jnk2*$^{-/-}$ cells were also demonstrated by immunofluorescence microscopy using Tom20 antibody (Fig. 1e, f) and transmission electron microscopy (Fig. 1g). Ectopic expression of HA-Jnk2 restored the mitophagy in *Jnk2*$^{-/-}$ MEFs (Supplementary Fig. 1h–j), suggesting that loss of Jnk2, rather than other genetic alterations, is responsible for the defective mitophagy. Furthermore, *Jnk2*$^{-/-}$ MEFs produced excessive mitochondrial ROS, an indication of accumulation of damaged mitochondria (Fig. 1h). Note, the general autophagic activity induced by hypoxia and HBSS was not altered by loss of Jnk2, as analyzed by the formation of LC3(II) (Supplementary Fig. 1k). Taken together, these data suggest that Jnk2 is required for stress-induced mitophagy.

Jnk2 is essential to maintain p62 abundance at steady-state

The initiation of mitophagy is mediated by PINK1 stabilization and Parkin translocation to the mitochondrial outer membrane[6–9]. We examined these two events in wild-type and *Jnk2*$^{-/-}$ MEFs under hypoxic conditions or following CCCP treatment. There were no significant differences in PINK1 stabilization (Supplementary Fig. 2a, b) and Parkin mitochondrial recruitment (Supplementary Fig. 2c) between wild-type and *Jnk2*$^{-/-}$ MEFs under hypoxic conditions or treated with CCCP. The mitophagy adaptor protein p62 is specifically required to mediate mitophagy but is dispensable for general autophagy[1,2,6,8,10–17]. We wondered whether Jnk2 might regulate mitophagy by affecting p62 expression. As expected, expression of p62 was significantly reduced in wild-type fibroblasts under hypoxic conditions or upon stimulation by CCCP or HBSS (Fig. 2a–c), consistent with previous reports that p62 is degraded together with enveloped cytosolic contents in the autolysosome during autophagy[17]. Interestingly, the steady-state abundance of p62 was severely decreased in *Jnk2*$^{-/-}$ MEFs (Fig. 2a–c). Similar results were obtained when Jnk2 was silenced by its specific siRNA (Fig. 2d). Conversely, ectopic expression of HA-Jnk2 restored the steady-state abundance of p62 in *Jnk2*$^{-/-}$ MEFs (Fig. 2e). Under our experimental conditions, p62 was required for mitophagy induced by hypoxia, CCCP or HBSS, as evidenced by the observation that silencing of p62 significantly inhibited Tom20 degradation in response to hypoxia, CCCP and HBSS (Fig. 2f–h). More importantly, ectopic

expression of Xpress-tagged p62 restored Tom20 degradation in *Jnk2*$^{-/-}$ MEFs in response to hypoxia, CCCP or HBSS (Fig. 2i–k). Thus, these data demonstrate that loss of Jnk2 significantly reduces the steady-state abundance of p62, resulting in defective mitophagy upon stress.

Jnk2 suppresses excessive autophagy in the steady state

p62 is degraded together with enveloped cytosolic contents in the autolysosome during autophagy induction, thereby serving as a marker of autophagy. The steady-state abundance of p62 is strictly regulated by degradation by the steady-state autophagy[1,2,16,20,22–29,37]. We tested whether loss of Jnk2 triggers more autophagy during basal conditions to enhance degradation of the steady-state p62, resulting in subsequently defective mitophagy upon stress. Real-time RT-PCR revealed that the mRNA abundance of p62 was comparable between wild-type and *Jnk2*$^{-/-}$ fibroblasts (Supplementary Fig. 3). However, treatment of *Jnk2*$^{-/-}$ MEFs with bafilomycin A1 led to accumulation of p62 to amounts comparable with those in wild-type fibroblasts cultured under similar conditions (Fig. 3a), indicating that there is an enhanced lysosomal degradation of p62 in the absence of Jnk2. Consistently, LC3-II formation and GFP-LC3 punctation were increased in *Jnk2*$^{-/-}$ MEFs when compared with wild-type fibroblasts under unstimulated conditions (Fig. 3b, c). Similar results were obtained when Jnk2 was silenced by its specific siRNA (Fig. 3d). Ectopic expression of HA-Jnk2 in *Jnk2*$^{-/-}$ MEFs reduced the steady-state autophagy activity to a level similar to that observed in wild-type fibroblasts (Fig. 3e). Furthermore, silencing of the essential autophagy-associated genes, *Becn1* (which encodes Beclin 1) or *Atg5*, restored p62 protein expression in *Jnk2*$^{-/-}$ MEFs (Fig. 3f, g). These data together suggest that increased steady-state autophagy activity in *Jnk2*$^{-/-}$ MEFs is responsible for the reduced steady-state expression of p62, thereby preventing the cells from mounting an efficient mitophagy upon stress.

Loss of Jnk2 stabilizes smARF proteins

The higher steady-state autophagy activity in *Jnk2*$^{-/-}$ MEFs may result from increased expression of pro-autophagy genes such as *Becn1* and *Atg5*. This possibility is not the case, since there was no detectable difference in the protein abundance of Beclin 1 or ATG5 between wild-type and *Jnk2*$^{-/-}$ fibroblasts (Supplementary Fig. 4a). Recently it was reported that overexpression of smARF potently induced autophagy and mitophagy[19]. We found that expression of smARF proteins was barely detectable in wild-type fibroblasts (Fig. 4a), consistent with previous reports that smARF is quickly turned over through proteasomal degradation in the steady state[19]. By contrast, the protein abundance of smARF was substantially increased in *Jnk2*$^{-/-}$ MEFs in the steady state (Fig. 4a). The identity of smARF in *Jnk2*$^{-/-}$ MEFs was validated by several approaches. First, two ARF siRNAs targeting different positions on its mRNA were able to reduce expression of both full length ARF (p19ARF) and smARF in *Jnk2*−/− MEFs (Supplementary Fig. 4b). Second, immunoblotting analysis using an additional ARF antibody against the C-terminus of ARF also revealed the accumulation of smARF in *Jnk2*$^{-/-}$ MEFs (Supplementary Fig. 4c). Finally, mass spectrometric analysis of smARF proteins immunoprecipitated from *Jnk2*$^{-/-}$ MEFs recovered a peptide with the sequence of LPGHAGGAAR, which is part of p19ARF and smARF (Supplementary Fig. 4d). The accumulated smARF was targeted exclusively to the

mitochondria in *Jnk2*$^{-/-}$ MEFs (Fig. 4b), consistent with previous reports that smARF is localized to mitochondria[19]. Similar results were obtained by silencing of Jnk2 but not Jnk1 (Fig. 4c and Supplementary Fig. 4e). Silencing of Jnk2 also enhanced the abundance of exogenous Xpress-tagged smARF (Supplementary Fig. 4f). Conversely, expression of exogenous HA-Jnk2 significantly reduced smARF protein abundance in *Jnk2*$^{-/-}$ MEFs (Fig. 4d).

Next we determined whether the kinase activity of Jnk2 is required for its regulation of smARF. Like wild-type Jnk2, expression of two kinase activity-deficient mutants of Jnk2, Jnk2(APF) or Jnk2(KM), reduced the amount of smARF protein in *Jnk2*$^{-/-}$ MEFs (Fig. 4e), suggesting that the kinase activity of Jnk2 is not required for its regulation of smARF expression. Previously, we showed that Jnk1 activity is enhanced in *Jnk2*$^{-/-}$ MEFs in unstimulated cells[26]. It is plausible that accumulated smARF proteins in *Jnk2*$^{-/-}$ MEFs are the result of increased Jnk1 activity. However silencing of Jnk1 in *Jnk2*$^{-/-}$ MEFs did not affect smARF protein expression (Supplementary Fig. 4g). Thus, Jnk enzymatic activity is not involved in the regulation of smARF protein stability.

To determine whether increased smARF abundance is responsible for the enhanced degradation of the steady-state p62 in *Jnk2*$^{-/-}$ MEFs, we silenced ARF in *Jnk2*$^{-/-}$ MEFs. Since smARF is the product of alternative translational initiation of ARF, ARF siRNA will target both full length p19ARF and smARF. To avoid the influence of ARF siRNA on the expression of full-length p19ARF, we transfected *Jnk2*$^{-/-}$ MEFs with ARF siRNA at a relatively low dose (20 nM) that significantly decreased expression of smARF but not the full-length p19ARF (Fig. 4f, g). Under this condition, p62 proteins were stabilized (Fig. 4f), while the enhanced formation of LC3-II and GFP-LC3 punctation was diminished in *Jnk2*$^{-/-}$ MEFs (Fig. 4g, h). Thus, smARF may account for the higher autophagic activity and lower p62 abundance in *Jnk2*$^{-/-}$ MEFs in the steady state. To further support this notion, *Arf*$^{-/-}$ MEFs were transfected with an expression vector encoding p19ARF, which generates full-length p19ARF and smARF proteins, or smARF (Fig. 4i). As expected, p62 protein expression was increased in *Arf*$^{-/-}$ MEFs compared to wild-type MEFs, but were reduced to amounts similar to those in wild-type fibroblasts in *Arf*$^{-/-}$ MEFs expressing smARF (Fig. 4i). However, complementation of *Arf*$^{-/-}$ cells with ARF(M45I), in which Met45 was substituted by Ile and thereby only generating full-length p19ARF, did not reduce the steady-state abundance of p62 (Supplementary Fig. 4h). Furthermore, silencing of smARF restored mitophagy in *Jnk2*$^{-/-}$ MEFs in response to hypoxia, CCCP and HBSS (Fig. 4j). Finally, in *Arf*$^{-/-}$ MEFs, the steady-state expression of p62 and stress-induced mitophagy were no longer affected by silencing of Jnk2 (Supplementary Fig. 4i). Taken together, these data suggest that stabilization of smARF in the absence of Jnk2 is mainly responsible for the excessive autophagy activity and subsequently lysosomal degradation of p62 in the steady state, leading to defective mitophagy under stress.

Jnk2 promotes smARF ubiquitination and degradation

The steady-state expression of smARF was extremely low in wild-type fibroblasts and only became detectable when cells were treated with the proteasome inhibitor MG-132 but not bafilomycin A1 (Fig. 5a and Supplementary Fig. 5a), consistent with the previous report that

smARF is rapidly degraded by the proteasome in unstimulated cells[19]. By contrast, MG-132 was unable to further increase smARF protein abundance in *Jnk2*$^{-/-}$ MEFs (Fig. 5a). This finding is not the result of defect in proteasome activity in *Jnk2*$^{-/-}$ fibroblasts, as shown by the hypoxia-inducible factor 1-alpha (HIF-1α) abundance before and after hypoxia treatment, as well as TNF-induced IκBα degradation (Supplementary Fig. 5b, c). The half-life of smARF in *Jnk2*$^{-/-}$ MEFs was much longer than that in wild-type fibroblasts (Fig. 5b), and the rapid turnover of smARF in wild-type fibroblasts was inhibited by MG-132 (Fig. 5c). These data suggest that Jnk2 promotes the proteasomal degradation of the steady-state smARF.

To determine whether Jnk2 triggers smARF for ubiquitination-dependent proteasomal degradation, wild-type fibroblasts that stably express Xpress-tagged smARF were transfected with siRNA against Jnk2 or control siRNA. Ubiquitination of Xpress-tagged smARF was analyzed by immunoprecipitation with the Xpress antibody followed by immunoblotting with a pan-ubiquitin or the K48-linkage specific ubiquitin antibody. Silencing of Jnk2 significantly decreased K48-linked polyubiquitination of smARF (Fig. 5d, e). Co-immunoprecipitation assays showed that smARF specifically interacted with ectopically expressed Jnk2 but not Jnk1 (Fig. 5f and Supplementary Fig. 5d), as well as endogenous Jnk2 (Fig. 5g). Jnk2 partially localized in mitochondria, where smARF exclusively resides, in the steady state (Supplementary Fig. 5e), suggesting that Jnk2 may target smARF for proteasomal degradation in mitochondria. Although Jnk2 also interacted with full-length p19ARF (Supplementary Fig. 5f), it did not affect p19ARF ubiquitination (Supplementary Fig. 5g). Taken together, these data suggest that Jnk2 facilitates K48-linked polyubiquitination of smARF to promote its proteasomal degradation.

Jnk2 prevents hypoxia-induced tissue damage

To understand the role of Jnk2 in stress-induced mitophagy, we used hypoxia as an *in vivo* model. Wild-type and *Jnk2*$^{-/-}$ mice were exposed to normoxia (21% O_2) or hypoxia (7% O_2) for 1, 4, and 7 days. The expression of Tom20 protein gradually decreased in the heart and lungs of hypoxic wild-type mice (Fig. 6a, b). By contrast, Tom20 degradation was inhibited in the heart and lungs of hypoxic *Jnk2*$^{-/-}$ mice (Fig. 6a, b). Dual immunofluorescence staining of heart and lungs from hypoxic wild-type mice showed the colocalization of LC3 puncta with mitochondria, which was severely decreased in *Jnk2*$^{-/-}$ mice (Fig. 6c, d). Histology analysis revealed that there was obvious damage in the heart and lungs of hypoxic *Jnk2*$^{-/-}$ mice compared with wild-type mice (Fig. 6e, f). We also observed less p62 protein and more accumulated smARF in the heart and lungs of *Jnk2*$^{-/-}$ mice compared with wild-type mice in the steady state (Supplementary Fig. 6a, b). Together, these data indicate that Jnk2 functions as a guardian to protect organs such as heart and lung from hypoxia-induced damage through promotion of mitophagy.

Jnk2 suppresses inflammasome activation

Defective mitophagy has been reported to induce excessive mitochondrial ROS, leading to inflammasome hyperactivation and elaboration of mature interleukin 1β (IL-1β)[3–5]. To determine the role of Jnk2-mediated mitophagy in the regulation of inflammasome activation, bone marrow-derived macrophages (BMDMs) were isolated from wild-type and

Jnk2$^{-/-}$ mice, primed with lipopolysaccharide (LPS), and then stimulated with ATP to activate inflammasomes[5]. Under this condition, *Jnk2*$^{-/-}$ macrophages secreted significantly more IL-1β and IL-18, as well as active, cleaved caspase-1 and IL-1β than wild-type macrophages (Fig. 7a, b). The enhanced inflammasome activity in *Jnk2*$^{-/-}$ macrophages was not the result of altered activation of the upstream signaling pathways, including NF-κB, p38 and Erk, as activation of these pathways was comparable between wild-type and *Jnk2*$^{-/-}$ macrophages (Supplementary Fig. 7a). Consistently, treatment with LPS plus ATP induced mitophagy in wild-type but not in *Jnk2*$^{-/-}$ macrophages, as analyzed by immunoblotting with Tom20 antibody and the colocalization of LC3 puncta with mitochondria (Fig. 7c, d). Under the same conditions, the amount of mitochondrial ROS in *Jnk2*$^{-/-}$ macrophages was increased when compared to wild-type cells (Fig. 7e). Treatment with the mitochondria-targeted antioxidant Mito-TEMPO, a scavenger specific for mitochondrial ROS[5], abrogated the increase in IL-1β and IL-18 secretion in *Jnk2*$^{-/-}$ macrophages in response to LPS plus ATP (Fig. 7f). Furthermore, ectopic expression of p62 inhibited the enhanced secretion of IL-1β and IL-18 in *Jnk2*$^{-/-}$ macrophages in response to LPS and ATP (Fig. 7g and Supplementary Fig. 7b). The partial inhibition of the enhanced secretion of IL-1β and IL-18 in *Jnk2*$^{-/-}$ macrophages by p62 is most likely due to the relatively low transduction efficiency of the p62-expressing lentivirus (~30%). Silencing of Jnk2 in murine alveolar macrophage cell line MH-S also enhanced the secretion of IL-1β and IL-18 in response to LPS plus ATP (Supplementary Fig. 7c). Similarly, addition of the inhibitor of the mitochondrial respiratory complex I rotenone or complex III Antimycin A induced more secretion of IL-1β and IL-18 and/or production of mitochondrial ROS in LPS-primed *Jnk2*$^{-/-}$ macrophages than in wild-type macrophages (Supplementary Fig. 7d, e).

To further determine the *in vivo* relevance of Jnk2 regulation of inflammasome activation, we used an animal model of endotoxic shock. Consistent with the *in vitro* results, serum concentrations of IL-1β and IL-18 were significantly higher in endotoxemic *Jnk2*$^{-/-}$ mice than in wild-type mice (Fig. 7h). *Jnk2*$^{-/-}$ mice were more susceptible to LPS-induced mortality than wild-type mice (Fig. 7i). *Jnk2*$^{-/-}$ macrophages also had less p62 protein and accumulated smARF in the steady state when compared with wild-type macrophages (Supplementary Fig. 7f). Together these data demonstrate that loss of Jnk2 results in inflammasome hyperactivation.

Jnk2 is not required for erythroid maturation

Mitophagy is critical for the coordinated removal of mitochondria during the terminal differentiation of erythrocytes. We found that red blood cell (RBC) counts, hemoglobin and hematocrit in the peripheral blood were similar between wild-type and *Jnk2*$^{-/-}$ mice (Supplementary Fig. 7g). We also examined RBCs for the expression of the erythroid cell marker Ter119, and the transferrin receptor CD71 that is down-regulated during terminal erythrocyte differentiation. The percentages of Ter119^{+}CD71^{+} reticulocytes and CD71^{-} mature erythrocytes from the blood were also similar between wild-type and *Jnk2*$^{-/-}$ mice (Supplementary Fig. 7h). In addition, there were comparable populations of Mitotracker Green (MTG) negative and CD71^{-} RBCs as well as MTG^{+}CD71^{+} RBCs between wild-type and *Jnk2*$^{-/-}$ mice (Supplementary Fig. 7i). These data suggest that loss of Jnk2 does not

affect erythrocyte differentiation in the steady state, implying differential roles of Jnk2 in mitophagy under stress and developmental conditions.

DISCUSSION

Overwhelming evidence shows that mitophagy has a fundamental role in many physiological events, from development to aging, and its deregulation contributes to many diseases including neurodegenerative diseases and immune disorders[1–5]. Although a series of key players in the mitophagy machinery have been identified[6–8], the regulatory mechanism of mitophagy remains largely unknown. In this report, we demonstrate that Jnk2 is required for stress-induced mitophagy through promotion of ubiquitination-dependent proteasomal degradation of smARF. Loss of Jnk2 results in tissue damage under hypoxic stress, as well as inflammasome hyperactivation and increased mortality in sepsis. Thus, Jnk2 functions as a guardian for organ integrity and thereby determines life or death under environmental stress.

Jnk2 positively regulates stress-induced mitophagy through targeting smARF for degradation independently of its kinase activity. Previously, it has been reported that Jnk1 is involved in starvation-induced autophagy through phosphorylation of Bcl-2 and inhibition of its association with Beclin 1 (ref. 32). Our results provide genetic evidence that Jnk2, but not Jnk1, targets smARF for ubiquitination-dependent proteasomal degradation in the steady-state in a kinase activity-independent manner, thereby ensuring cells to mount an efficient mitophagy to eliminate damaged mitochondria under stress *in vitro* and *in vivo*. Although the underlying mechanism by which Jnk2 targets smARF for ubiquitination has yet to be determined, our observation that Jnk2 interacts with smARF suggests that Jnk2 may act as an adaptor to facilitate the interaction of smARF with its E3 ligase. The cellular compartment where Jnk2 targets smARF for proteasomal degradation also remains to be determined. However, our results show that Jnk2 can localize to the mitochondria, where smARF exclusively resides. Therefore, it is possible that Jnk2 may target smARF for proteasomal degradation in mitochondria. Although Jnk2 also interacted with full length p19ARF, it did not affect p19ARF ubiquitination. It is possible that the N-terminal region of p19ARF, which mediates its binding to many cofactors but is missing in smARF[38,39], may interfere with Jnk2-mediated ubiquitination of p19ARF. Although p19ARF contributes to autophagy when overexpressed or under pathological conditions such as oncogenic stress or in cancer cells[22,40,41], the slightly increased p19ARF in *Jnk2*$^{-/-}$ cells is less likely accountable for the higher autophagic activity and decreased p62 expression in the steady state, as complementation of *Arf*$^{-/-}$ cells with ARF(M45I) did not reduce the steady-state abundance of p62. Thus, smARF may play a dominant role in the higher autophagic activity in Jnk2 KO cells.

The Ub- and LC3-binding adaptor protein p62 is essential for Jnk2 to promote stress-induced mitophagy. The role of p62 in mitophagy has been controversial. While it has been reported that p62 is critical for removal of depolarized mitochondria via mitophagy[1,2,6,8,11–16], it has also been shown that p62 is dispensable for mitophagy, possibly due to the redundancy with a related Ub- and LC3-binding protein NBR1 (refs. 2, 42). Our results show that loss of Jnk2 enhanced lysosomal degradation of the steady-state

p62, resulting in defective mitophagy upon stress, while ectopic expression of p62 in *Jnk2*$^{-/-}$ MEFs restored mitophagy in response to stresses. Consistently, silencing of p62 resulted in defective mitophagy upon cellular stresses. Thus, our studies demonstrate that p62 plays a crucial role in Jnk2-mediated regulation of mitophagy upon stress.

smARF has a dual function in autophagy/mitophagy. Previous studies have shown that ectopic over-expression of smARF is able to induce mitochondria depolarization and autophagy/mitophagy[19]. However, the pathophysiological function of endogenous smARF is not known. Our results show that loss of Jnk2 induced accumulation of smARF, resulting in higher steady-state autophagy in unstimulated cells, consistent with previous studies obtained from ectopic over-expression of smARF[19]. Paradoxically, our results reveal that accumulated endogenous smARF in the absence of Jnk2 enhanced the steady-state autophagy that caused enhanced lysosomal degradation of p62, resulting in defective stress-induced mitophagy. Thus, accumulated endogenous smARF in the absence of Jnk2 regulates autophagy/mitophagy in two distinct but interrelated mechanisms: promotion of the steady-state autophagy and suppression of stress-induced mitophagy.

We observed slightly more Tom20 protein at baseline in Jnk2-deficient cells, which was not rescued by overexpression of p62. In addition, silencing of Jnk2 in *Arf*$^{-/-}$ MEFs still resulted in more Tom20 without a decrease in p62 abundance in the steady state. By contrast, either ectopic expression of p62 or silencing of smARF restored Tom20 degradation in Jnk2 KO cells in response to mitophagy inducers, regardless of the basal amount of Tom20. Moreover, in *Arf*$^{-/-}$ MEFs, stress-induced Tom20 degradation or the steady-state expression of p62 was not affected by silencing of Jnk2, albeit an increase in basal Tom20 abundance caused by knockdown of Jnk2 in these cells. Therefore, Jnk2 regulates stress-induced mitophagy via the smARF-p62 axis. It is likely that Jnk2 regulates basal Tom20 expression through a different mechanism, but this regulation is unlikely involved in Jnk2 regulation of stress-induced mitophagy.

Jnk2 is not required for erythroid maturation. It is known that mitophagy is critical for mitochondrial elimination during erythroid maturation[43]. Our findings that Jnk2 is critical for mitophagy under stress conditions but not during erythroid maturation indicate that Jnk2 differentially regulates mitophagy under stress and developmental conditions. During reticulocyte maturation, it is possible that either Jnk2-maintained p62 is not required for this type of mitophagy or that its deficiency is compensated by other pathways, such as Nix, a mitochondrial protein that is able to directly bind to LC3 and is significantly upregulated during terminal erythroid differentiation[43].

Our finding identifies Jnk2 as a novel key regulator of inflammasome activation. Our results show that *Jnk2*$^{-/-}$ macrophages, which had defective stress-induced mitophagy and excessive ROS, had increased secretion of IL-1β and IL-18, as well as active caspase-1 and IL-1β in response to LPS and ATP. More importantly, *Jnk2*$^{-/-}$ mice had increased concentrations of serum IL-1β and IL-18 and higher mortality rate, accompanied by impaired clearance of damaged mitochondria, compared to wild-type mice in a mouse model of sepsis. Thus, promotion of stress-activated mitophagy by Jnk2 may play a critical role in prevention of inflammasome hyperactivation. Sepsis represents an exaggerated systemic

inflammatory response to infection that can progress to multi-organ failure including shock[44,45]. Up to date there is no effective treatment for sepsis. It has long been considered that sepsis is a condition associated with mitochondrial dysfunction and a recent study of the metabolome and proteome in septic patients revealed that mitochondrial dysfunction can serve as a signature that indicates sepsis outcomes[46]. In support of this observation, a recent report showed that upregulation of autophagy not only inhibits inflammatory cytokine production, but also confers tissue tolerance to damage in sepsis, which may represent an efficacious therapeutic option for sepsis[47,48]. Thus, promotion of mitophagy by Jnk2 may protect organs from sepsis-induced damage by at least two interrelated mechanisms: suppression of inflammasome activation and conferring tissue tolerance to damage. Targeting both inflammation and tissue tolerance to damage by upregulating mitophagy may be critical for prevention of sepsis-induced tissue damage and organ failure. It will be of interest to investigate whether Jnk2 is dysregulated during sepsis in mice. Furthermore, targeting Jnk2-regulated mitophagy for tissue tolerance to damage may have broad applications to many other pathological conditions that are associated with mitochondrial dysfunction like sepsis.

METHODS

Mice

*Jnk*2$^{-/-}$ mice on the C57BL/6 background were kindly provided by M. Karin. The animal care and experiments were performed in compliance with the institutional and US National Institutes of Health guidelines and were approved by the Northwestern University Animal Care and Use Committee. For the mortality studies, when mice became moribund (hunched posture, lack of curiosity, little or no response to stimuli and not moving when touched), a clinically irreversible condition that leads to inevitable death, according to the guidelines for the selection of humane endpoints in rodent studies at Northwestern University, they were sacrificed.

MEFs and treatment

Jnk1- or Jnk2-deficient MEFs were previously described[26]. Cells were exposed to normoxia (21% O_2) or hypoxia (7% O_2), or treated with CCCP (5 μM), or starved by incubation in HBSS, as indicated.

Reagents

TNF was from R&D Systems. LPS (L2630), Antimycin A, CCCP, Rotenone, Mito-TEMPO, bafilomycin A1, MG132, and CHX were from Sigma-Aldrich. ATP was from ENZO Life Sciences. TMRE, MitoTracker Deep Red, MitoTracker Green and MitoSox Red were from Life technologies. HBSS was from Cellgro. The ProcartaPlex Mouse Basic kit, mouse IL-1β Simplex and IL-18 Simplex were from eBioscience. Monoclonal antibodies used in this study are listed in Supplementary Table 1. The mCherry-Parkin plasmid was a gift from Richard Youle (Addgene plasmid # 23956)[1,2]. The following siRNA oligos were from Thermo Scientific (Dharmacon products): control siRNA (D-001210-02); ARF siRNA # 1 (5′-AGGUGAUGAUGAUGGGCAATT-3′); ARF siRNA # 2 (5′-GGUCGCAGGUUCUUGGUCATT-3′); p62 siRNA (L-047628-01); Jnk2 siRNA (5′-

CCGCAGAGUUCAUGAAGAATT-3′); Jnk1 siRNA (5′-UGAUUCAGAUGGAGUUAGATT-3′); Beclin 1 (5′-CAGUUUGGCACAAUCAAUATT-3′); ATG5 siRNA (5′-CAUCAACCGGAAACUCAUTT-3′).

Lentivirus infection

Cells (3×10^5) were infected with 0.5 ml lentivirus stock (10^7–10^8 transduction units/ml) twice every 6 h. Cells were washed once between the infections by adding cell culture medium for 30 min, as we previously described[49].

In vivo experiments

For hypoxic mouse model, female WT or *Jnk2*$^{-/-}$ mice (6–8 weeks old) were exposed to normoxia (21% O_2) or hypoxia (7% O_2) for 1, 4 or 7 days. Heart and lungs were harvested and the homogenates were lysed in RIPA buffer to prepare protein extracts for immunoblotting in a subgroup of mice. In another subgroup of mice, heart and lung tissues were fixed, embedded in paraffin and analyzed by H&E staining. For mouse model of sepsis, mice were injected intraperitoneally with *Escherichia coli* LPS (12 mg/kg; or 34 mg/kg for mortality studies).

Analysis of cytokines

The concentrations of cytokines, including IL-1β and IL-18, in the cell culture supernatants or mouse serum were determined using the multiplex immunoassay (eBioscience).

Isolation and culture of mouse BMDMs

BMDMs were isolated as we previously described[50]. Briefly, bone marrow cells collected from mouse femurs were plated on petri dishes and cultured for 5 d in DMEM containing 10% FBS with 2 mM L-glutamine, 100 units/ml penicillin, 100 μg/ml streptomycin, and 25% conditioned medium from L929 mouse fibroblasts.

Analysis of inflammasome activation

Cells were primed with LPS (10 ng/ml) for 16 h followed by treatment with ATP (2 mM) for 1 h, or rotenone (40 μM) or Antimycin A (10 μg/ml) for 6 h. Supernatants were collected for cytokine analysis or precipitated for immunoblotting with Caspase-1 or IL-1β antibody. Cells were lysed for immunoblotting with Caspase-1 or IL-1β antibody. In some experiments, cells were pre-treated with Mito-TEMPO (200 μM) for 1 h before treatment with LPS and ATP, as indicated in figure legends.

Mitochondrial ROS measurement

Cells were stained with MitoSOX (5 μM) for 15 min at 37 °C. Cells were then washed with PBS, trypsinized and suspended in PBS containing 1% FBS. Data were acquired with BD LSRFortessa Analyzer and were analyzed with FlowJo analytical software (TreeStar).

Transmission electron microscopy

Cells were fixed in 4% formaldehyde and 1% glutaraldehyde, and then processed for transmission electron microscopy by the Northwestern University Cell Imaging Facility.

Generation of stable cell lines and siRNA transfection

WT or *Jnk2*$^{-/-}$ MEFs were transfected with pEGFP-LC3 vector encoding GFP-LC3 or pcDNA3.1 vector encoding Xpress-tagged smARF. Two d after the transfection, cells were selected by G418 (300 μg/ml). For the siRNA transfections, the cells were transfected with siRNAs (100 nM).

Fluorescence microscopy

GFP-LC3-expressing stable cells were incubated with MitoTracker Deep Red (100 nM) for 30 min at 37 °C and then fixed with ice-cold methanol, and mounted in DAPI-containing solution, followed by fluorescence microscopy, as indicated in figure legends. In some experiments, cells were incubated with MitoTracker Deep Red, and then fixed and permeabilized by subsequent incubations in ice-cold methanol and 0.02% NP40. Cells were then subjected to immunofluorescence staining using Tom20 or LC3 antibody, as indicated in figure legends. For immunofluorescence staining of tissues, paraffin-embedded sections were deparaffinized and processed for double immunofluorescence staining using LC3 and Tom20 antibodies by the Northwestern University Pathology Core Facility.

Cell fractionation

Cells were fractionated into cytoplasmic (cytosolic+mitochondrial) and nuclear fractions using the NE-PER Nuclear and Cytoplasmic Extraction Kit (Thermo Scientific), or cytosolic and mitochondrial fractions using the Mitochondria/Cytosol Fractionation Kit (BioVision), according to the manufacturer's instructions.

Mass spectrometry

Mass spectrometry analysis was done by K. Stone at the Mass Spectrometry Core Facility at Yale University.

Flow Cytometry

Erythroid cells from peripheral blood were labeled with 50 nM Mitotracker Green at 37 °C for 30 min. The cells were then stained with anti-Ter119-PE and anti-CD71-APC, followed by flow cytometry.

Statistical analysis

Data were analyzed by an unpaired Student's *t*-test or Log-rank Test as indicated, with the assumption of normal distribution of data and equal sample variance. Sample sizes were selected on the basis of preliminary results to ensure an adequate power. All cells and mice used for the study were included for the statistical analysis, with no randomization or blinding involved. No exclusion of data points was used.

Supplementary Material

Refer to Web version on PubMed Central for supplementary material.

Acknowledgments

We thank M. Karin (University of California, San Diego) for kindly providing us with *Jnk2*$^{-/-}$ mice; Y. Cheng and M. A. Baker for help with the analysis of inflammasome activation; and A. Yemelyanov for lentivirus preparation. Supported by the US National Institutes of Health Grants HL114763 (to J.L.) and American Asthma Foundation Scholar Award 13-0114 (to J.L.).

References

1. Youle RJ, Narendra DP. Mechanisms of mitophagy. Nat Rev Mol Cell Biol. 2011; 12:9–14. [PubMed: 21179058]
2. Ding WX, Yin XM. Mitophagy: mechanisms, pathophysiological roles, and analysis. Biol Chem. 2012; 393:547–564. [PubMed: 22944659]
3. Lupfer C, et al. Receptor interacting protein kinase 2-mediated mitophagy regulates inflammasome activation during virus infection. Nat Immunol. 2013; 14:480–488. [PubMed: 23525089]
4. Zhou R, Yazdi AS, Menu P, Tschopp J. A role for mitochondria in NLRP3 inflammasome activation. Nature. 2011; 469:221–225. [PubMed: 21124315]
5. Nakahira K, et al. Autophagy proteins regulate innate immune responses by inhibiting the release of mitochondrial DNA mediated by the NALP3 inflammasome. Nat Immunol. 2011; 12:222–230. [PubMed: 21151103]
6. Hollville E, Carroll RG, Cullen SP, Martin SJ. Bcl-2 family proteins participate in mitochondrial quality control by regulating Parkin/PINK1-dependent mitophagy. Mol Cell. 2014; 55:451–466. [PubMed: 24999239]
7. Hasson SA, et al. High-content genome-wide RNAi screens identify regulators of parkin upstream of mitophagy. Nature. 2013; 504:291–295. [PubMed: 24270810]
8. Geisler S, et al. PINK1/Parkin-mediated mitophagy is dependent on VDAC1 and p62/SQSTM1. Nat Cell Biol. 2010; 12:119–131. [PubMed: 20098416]
9. Koyano F, et al. Ubiquitin is phosphorylated by PINK1 to activate parkin. Nature. 2014; 510:162–166. [PubMed: 24784582]
10. Moscat J, Diaz-Meco MT. p62 at the crossroads of autophagy, apoptosis, and cancer. Cell. 2009; 137:1001–1004. [PubMed: 19524504]
11. Lee JY, Nagano Y, Taylor JP, Lim KL, Yao TP. Disease-causing mutations in parkin impair mitochondrial ubiquitination, aggregation, and HDAC6-dependent mitophagy. J Cell Biol. 2010; 189:671–679. [PubMed: 20457763]
12. Okatsu K, et al. p62/SQSTM1 cooperates with Parkin for perinuclear clustering of depolarized mitochondria. Genes Cells. 2010; 15:887–900. [PubMed: 20604804]
13. Ding WX, et al. Nix is critical to two distinct phases of mitophagy, reactive oxygen species-mediated autophagy induction and Parkin-ubiquitin-p62-mediated mitochondrial priming. J Biol Chem. 2010; 285:27879–27890. [PubMed: 20573959]
14. Politi Y, et al. Paternal mitochondrial destruction after fertilization is mediated by a common endocytic and autophagic pathway in Drosophila. Dev Cell. 2014; 29:305–320. [PubMed: 24823375]
15. Geisler S, Vollmer S, Golombek S, Kahle PJ. The ubiquitin-conjugating enzymes UBE2N, UBE2L3 and UBE2D2/3 are essential for Parkin-dependent mitophagy. J Cell Sci. 2014; 127:3280–3293. [PubMed: 24906799]
16. Park S, Choi SG, Yoo SM, Son JH, Jung YK. Choline dehydrogenase interacts with SQSTM1/p62 to recruit LC3 and stimulate mitophagy. Autophagy. 2014; 10:1906–1920. [PubMed: 25483962]
17. Kirkin V, McEwan DG, Novak I, Dikic I. A role for ubiquitin in selective autophagy. Mol Cell. 2009; 34:259–269. [PubMed: 19450525]

18. Sahani MH, Itakura E, Mizushima N. Expression of the autophagy substrate SQSTM1/p62 is restored during prolonged starvation depending on transcriptional upregulation and autophagy-derived amino acids. Autophagy. 2014; 10:431–441. [PubMed: 24394643]
19. Reef S, et al. A short mitochondrial form of p19ARF induces autophagy and caspase-independent cell death. Mol Cell. 2006; 22:463–475. [PubMed: 16713577]
20. Reef S, Kimchi A. Nucleolar p19ARF, unlike mitochondrial smARF, is incapable of inducing p53-independent autophagy. Autophagy. 2008; 4:866–869. [PubMed: 18719357]
21. Budina-Kolomets A, Hontz RD, Pimkina J, Murphy ME. A conserved domain in exon 2 coding for the human and murine ARF tumor suppressor protein is required for autophagy induction. Autophagy. 2013; 9:1553–1565. [PubMed: 23939042]
22. Abida WM, Gu W. p53-Dependent and p53-independent activation of autophagy by ARF. Cancer Res. 2008; 68:352–357. [PubMed: 18199527]
23. Hibi M, Lin A, Smeal T, Minden A, Karin M. Identification of an oncoprotein- and UV-responsive protein kinase that binds and potentiates the c-Jun activation domain. Genes Dev. 1993; 7:2135–2148. [PubMed: 8224842]
24. Chang L, Karin M. Mammalian MAP kinase signalling cascades. Nature. 2001; 410:37–40. [PubMed: 11242034]
25. Davis RJ. Signal transduction by the JNK group of MAP kinases. Cell. 2000; 103:239–252. [PubMed: 11057897]
26. Liu J, Minemoto Y, Lin A. c-Jun N-terminal protein kinase 1 (JNK1), but not JNK2, is essential for tumor necrosis factor alpha-induced c-Jun kinase activation and apoptosis. Mol Cell Biol. 2004; 24:10844–10856. [PubMed: 15572687]
27. Sabapathy K, et al. Distinct roles for JNK1 and JNK2 in regulating JNK activity and c-Jun-dependent cell proliferation. Mol Cell. 2004; 15:713–725. [PubMed: 15350216]
28. Fuchs SY, Dolan L, Davis RJ, Ronai Z. Phosphorylation-dependent targeting of c-Jun ubiquitination by Jun N-kinase. Oncogene. 1996; 13:1531–1535. [PubMed: 8875991]
29. Fuchs SY, et al. c-Jun NH2-terminal kinases target the ubiquitination of their associated transcription factors. J Biol Chem. 1997; 272:32163–32168. [PubMed: 9405416]
30. Fuchs SY, Fried VA, Ronai Z. Stress-activated kinases regulate protein stability. Oncogene. 1998; 17:1483–1490. [PubMed: 9779995]
31. Fuchs SY, et al. JNK targets p53 ubiquitination and degradation in nonstressed cells. Genes Dev. 1998; 12:2658–2663. [PubMed: 9732264]
32. Wei Y, Pattingre S, Sinha S, Bassik M, Levine B. JNK1-mediated phosphorylation of Bcl-2 regulates starvation-induced autophagy. Mol Cell. 2008; 30:678–688. [PubMed: 18570871]
33. Wu W, et al. ULK1 translocates to mitochondria and phosphorylates FUNDC1 to regulate mitophagy. EMBO Rep. 2014; 15:566–575. [PubMed: 24671035]
34. Liu L, et al. Mitochondrial outer-membrane protein FUNDC1 mediates hypoxia-induced mitophagy in mammalian cells. Nat Cell Biol. 2012; 14:177–185. [PubMed: 22267086]
35. Guo JY, et al. Activated Ras requires autophagy to maintain oxidative metabolism and tumorigenesis. Genes Dev. 2011; 25:460–470. [PubMed: 21317241]
36. Bianchi ME. Killing cancer cells, twice with one shot. Cell Death Differ. 2014; 21:1–2. [PubMed: 24317270]
37. Li N, et al. Loss of acinar cell IKKalpha triggers spontaneous pancreatitis in mice. J Clin Invest. 2013; 123:2231–2243. [PubMed: 23563314]
38. Kuo ML, den Besten W, Bertwistle D, Roussel MF, Sherr CJ. N-terminal polyubiquitination and degradation of the Arf tumor suppressor. Genes Dev. 2004; 18:1862–1874. [PubMed: 15289458]
39. Chen D, Shan J, Zhu WG, Qin J, Gu W. Transcription-independent ARF regulation in oncogenic stress-mediated p53 responses. Nature. 2010; 464:624–627. [PubMed: 20208519]
40. Pimkina J, Murphy ME. ARF, autophagy and tumor suppression. Autophagy. 2009; 5:397–399. [PubMed: 19221462]
41. Balaburski GM, Hontz RD, Murphy ME. p53 and ARF: unexpected players in autophagy. Trends Cell Biol. 2010; 20:363–369. [PubMed: 20303758]

42. Narendra D, Kane LA, Hauser DN, Fearnley IM, Youle RJ. p62/SQSTM1 is required for Parkin-induced mitochondrial clustering but not mitophagy; VDAC1 is dispensable for both. Autophagy. 2010; 6:1090–1106. [PubMed: 20890124]
43. Sandoval H, et al. Essential role for Nix in autophagic maturation of erythroid cells. Nature. 2008; 454:232–235. [PubMed: 18454133]
44. Hotchkiss RS, Karl IE. The pathophysiology and treatment of sepsis. N Engl J Med. 2003; 348:138–150. [PubMed: 12519925]
45. Angus DC, van der Poll T. Severe sepsis and septic shock. N Engl J Med. 2013; 369:840–851. [PubMed: 23984731]
46. Langley RJ, et al. An integrated clinico-metabolomic model improves prediction of death in sepsis. Sci Transl Med. 2013; 5:195ra195.
47. Figueiredo N, et al. Anthracyclines induce DNA damage response-mediated protection against severe sepsis. Immunity. 2013; 39:874–884. [PubMed: 24184056]
48. Medzhitov R. Septic shock: on the importance of being tolerant. Immunity. 2013; 39:799–800. [PubMed: 24238335]
49. Do-Umehara HC, et al. Suppression of inflammation and acute lung injury by Miz1 via repression of C/EBP-delta. Nat Immunol. 2013; 14:461–469. [PubMed: 23525087]
50. Liu J, et al. Site-specific ubiquitination is required for relieving the transcription factor Miz1-mediated suppression on TNF-alpha-induced JNK activation and inflammation. Proc Natl Acad Sci U S A. 2012; 109:191–196. [PubMed: 22184250]

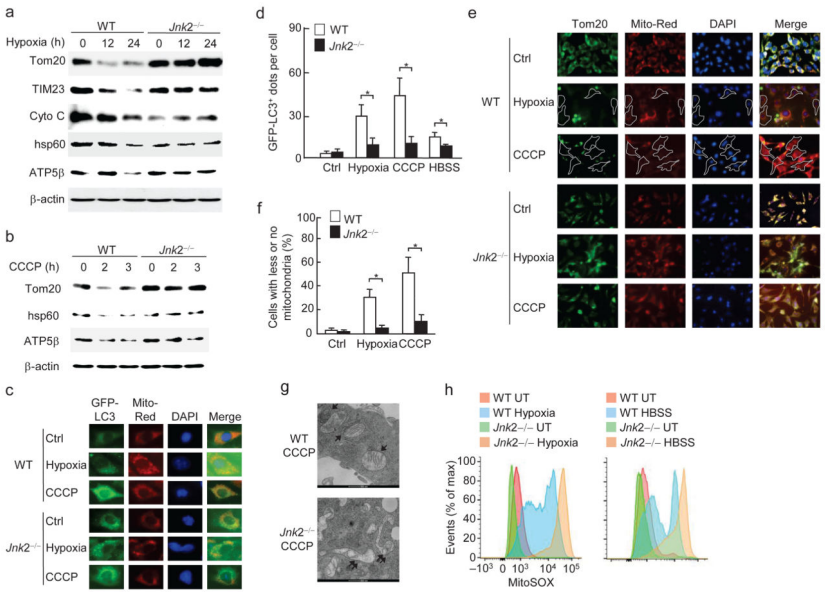

Figure 1. Jnk2 is required for stress-induced mitophagy

(**a**) WT and *Jnk2*$^{-/-}$ MEFs were exposed to normoxia (21% O_2) or hypoxia (1.5% O_2) for indicated times. Expressions of Tom20, TIM23, Cytochrome C, HSP60, ATP5β and β-actin were determined by immunoblotting. (**b**) WT and *Jnk2*$^{-/-}$ MEFs were treated with CCCP (5 μM) for indicated times. Expressions of Tom20, HSP60, ATP5β and β-actin were determined by immunoblotting. (**c, d**) Stable WT and *Jnk2*$^{-/-}$ MEFs expressing GFP-LC3 were subjected to hypoxia for 24 h or treated with CCCP for 3 h. Cells were analyzed for the co-localization of GFP-LC3 with mitochondria (Mitotracker Deep Red) using fluorescence microscopy (**c**). The numbers of GFP-LC3 puncta co-localized with mitochondria per cell were quantified (**d**). (**e, f**) WT and *Jnk2*$^{-/-}$ MEFs were exposed to hypoxia or treated with CCCP for 24 h. Cells were immunostained with anti-Tom20 followed by fluorescence microscopy (**e**). The percentage of cells with less/no mitochondria was quantified (**f**). (**g**) Transmission electron microscopy of WT and *Jnk2*$^{-/-}$ MEFs treated with CCCP for 24 h. Arrows: engulfed mitochondria in autophagosomes. Double arrows: swollen mitochondria with disrupted cristae. (**h**) Flow cytometry of hypoxia or HBSS-treated WT and *Jnk2*$^{-/-}$ MEFs stained with MitoSOX. UT, untreated. Data are representative of at least three independent experiments (**a–h**) (**d**, **f**; mean and s.e.m. of 100 cells over multiple microscopic fields (**d**), or 20 individual microscopic fields (**f**)). *, $P < 0.05$ by unpaired Student's *t*-test.

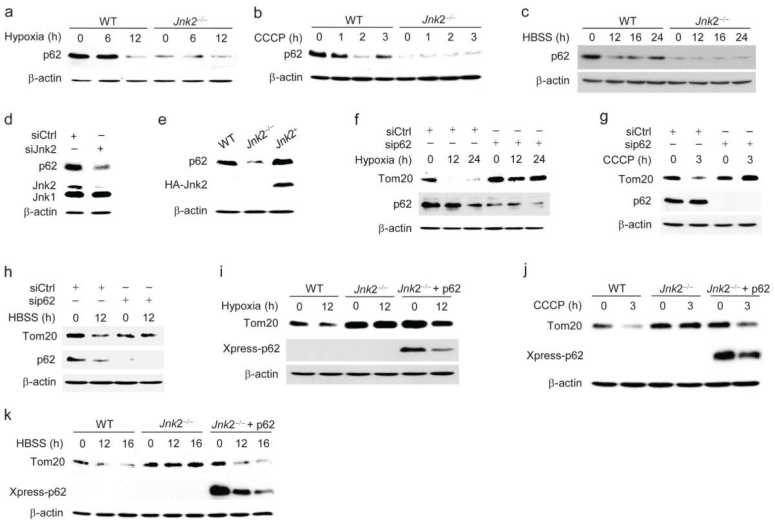

Figure 2. Loss of Jnk2 results in decreased steady-state levels of p62

(**a–c**) WT and *Jnk2*$^{-/-}$ MEFs were exposed to hypoxia (**a**), or treated with CCCP (**b**) or HBSS (**c**) for indicated times. The expression of p62 was determined by immunoblotting. (**d**) Expression of p62 in WT MEFs transfected with control siRNA or Jnk2 siRNA. (**e**) *Jnk2*$^{-/-}$ MEFs were transfected with expression vector encoding HA-Jnk2 or empty vector. Forty-eight h later, expressions of p62 and HA-Jnk2 were determined. WT MEFs were used as control. (**f–h**) WT MEFs were transfected with control siRNA or p62 siRNA. Thirty-six h later, cells were exposed to hypoxia (**f**), or treated with CCCP (**g**) or HBSS (**h**) for indicated times. Expressions of Tom20 and p62 were determined. (**i–k**) *Jnk2*$^{-/-}$ MEFs were transfected with expression vector encoding Xpress-tagged p62 or empty vector. Thirty-six h later, cells were exposed to hypoxia (**i**), or treated with CCCP (**j**) or HBSS (**k**) for indicated times. Expressions of Tom20 and Xpress-tagged p62 were determined. Data are representative of three independent experiments (**a–k**).

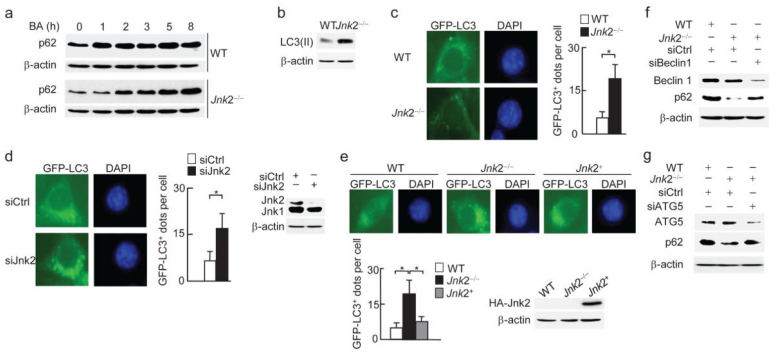

Figure 3. Loss of Jnk2 results in excessive steady-state autophagic activity

(**a**) WT and *Jnk2*$^{-/-}$ MEFs were treated with bafilomycin A1 for indicated times. Expression of p62 was assessed. BA, bafilomycin A1. (**b**) Formation of LC3(II) in WT and *Jnk2*$^{-/-}$ MEFs in the steady state assessed by immunoblotting. (**c**) Fluorescence microscopy of WT and *Jnk2*$^{-/-}$ MEFs stably transfected with GFP-LC3 (left). The numbers of GFP-LC3 puncta per cell were quantified (right). (**d**) Fluorescence microscopy and quantification of GFP-LC3 puncta in WT MEFs transfected with control siRNA or Jnk2 siRNA (left). Expression of Jnk2 was determined by immunoblotting (right). (**e**) Fluorescence microscopy and quantification of GFP-LC3 puncta in *Jnk2*$^{-/-}$ MEFs transfected with expression vector encoding HA-Jnk2 or empty vector. WT MEFs were used as control. Expression of HA-Jnk2 was determined by immunoblotting. (**f, g**) *Jnk2*$^{-/-}$ MEFs were transfected with control siRNA or Beclin 1 siRNA (**f**) or ATG5 siRNA (**g**). Expressions of p62 and Beclin 1 or ATG5 were determined. Data are representative of three independent experiments (**a–g**) (**c, d, e**; mean and s.e.m. of 100 cells over multiple microscopic fields). *, $P < 0.05$ by unpaired Student's *t*-test.

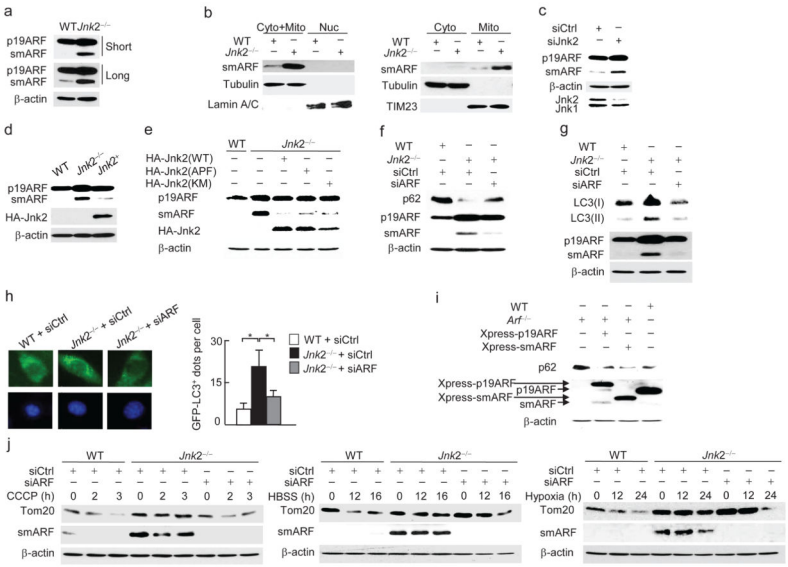

Figure 4. Loss of Jnk2 stabilizes smARF

(**a**) Immunoblotting analysis of WT and *Jnk2*$^{-/-}$ MEFs with ARF antibody (ab26696, Abcam). (**b**) WT and *Jnk2*$^{-/-}$ MEFs were fractionated into cytosolic+mitochondrial, nuclear, cytosolic or mitochondrial fractions. Expression of smARF was assessed by immunoblotting. Tubulin, Lamin A/C and TIM23 were used as markers for the cytoplasm, nucleus and mitochondria, respectively. (**c**) Expression of p19ARF and smARF in WT MEFs transfected with control siRNA or Jnk2 siRNA. (**d**) Expression of p19ARF and smARF in WT or *Jnk2*$^{-/-}$ MEFs transfected with expression vector encoding HA-Jnk2 or empty vector. (**e**) Expression of p19ARF and smARF in WT or *Jnk2*$^{-/-}$ MEFs transfected with HA-Jnk2(WT) or HA-Jnk2(APF) or HA-Jnk2(KM). (**f**) Expression of p62 in WT or *Jnk2*$^{-/-}$ MEFs transfected with control siRNA or ARF siRNA. (**g**) Formation of LC3(II) in WT or *Jnk2*$^{-/-}$ MEFs transfected with control siRNA or ARF siRNA. (**h**) Fluorescence microscopy of WT or *Jnk2*$^{-/-}$ MEFs transfected with control siRNA or ARF siRNA (left). The numbers of GFP-LC3 puncta per cell were quantified (right). (**i**) Expression of p62 in WT or *Arf*$^{-/-}$ MEFs transfected with expression vector encoding Xpress-tagged p19ARF or Xpress-tagged smARF or empty vector. (**j**) WT or *Jnk2*$^{-/-}$ MEFs were transfected with control siRNA or ARF siRNA as indicated. Thirty-six h later, cells were treated with CCCP, or HBSS, or exposed to hypoxia for indicated times. Expressions of Tom20 and smARF were determined. Data are representative of at least three independent experiments (**a–j**) (**h**; mean and s.e.m. of 100 cells over multiple microscopic fields). *, $P < 0.05$ by unpaired Student's *t*-test.

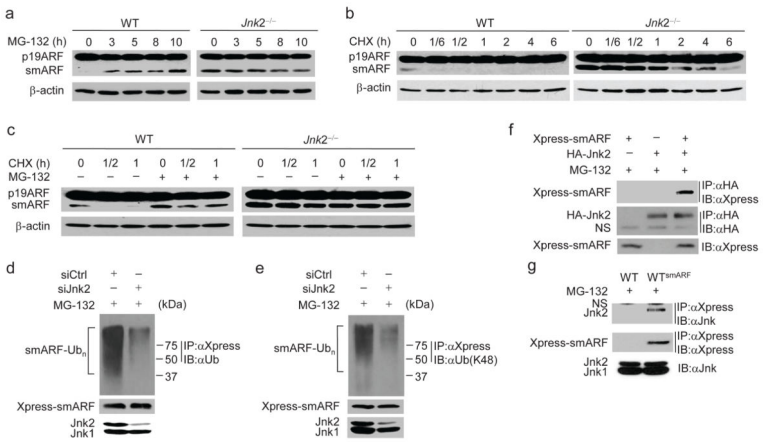

Figure 5. Jnk2 promotes smARF ubiquitination and degradation

(**a, b**) WT and *Jnk2*$^{-/-}$ MEFs were treated with MG-132 (**a**) or CHX (**b**) for indicated times. Expressions of p19ARF and smARF were determined. (**c**) WT and *Jnk2*$^{-/-}$ MEFs were treated with CHX for indicated times in the absence or presence of MG-132. Expressions of p19ARF and smARF were determined. (**d, e**) Stable WT MEFs expressing Xpress-tagged smARF were transfected with control siRNA or Jnk2 siRNA. Ubiquitination of Xpress-tagged smARF was determined by immunoprecipitation with anti-Xpress followed by immunoblotting with anti-ubiquitin (**d**) or K48-linkage specific ubiquitin antibody (**e**). (**f**) Co-immunoprecipitation of ectopic Xpress-tagged smARF and HA-Jnk2. (**g**) Co-immunoprecipitation of Xpress-tagged smARF and endogenous Jnk2 in WT MEFs stably expressing Xpress-tagged smARF (WT^{smARF}). WT MEFs were used as control. NS, non-specific. Data are representative of three independent experiments (**a–g**).

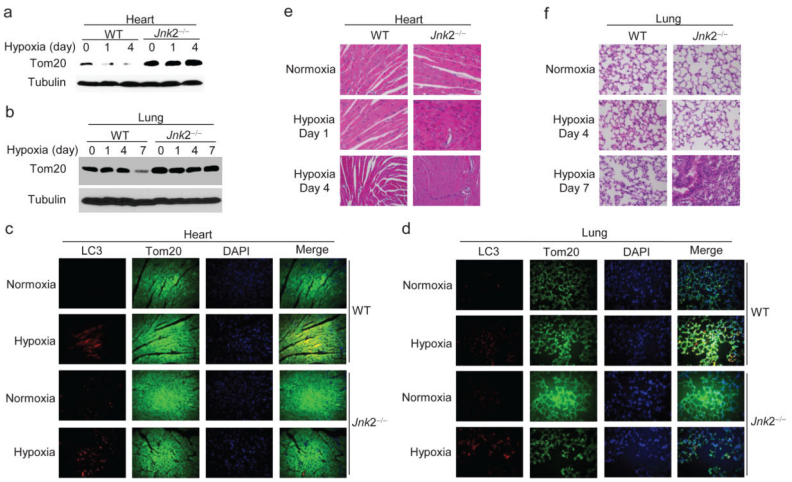

Figure 6. Jnk2 prevents hypoxia-induced tissue damage

(**a–f**) WT and *Jnk2*$^{-/-}$ mice were exposed to normoxia (21% O_2) or hypoxia (7% O_2) for indicated times. Expression of Tom20 in heart (**a**) and lungs (**b**) was determined by immunoblotting. Co-localization of LC3 puncta with mitochondria was assessed by double immunofluorescence with LC3 and Tom20 antibodies (**c, d**). Histology of heart (**e**) and lungs (**f**) was analyzed by H&E staining. Data are representative of three independent experiments with 6–7 mice per group (**a–f**).

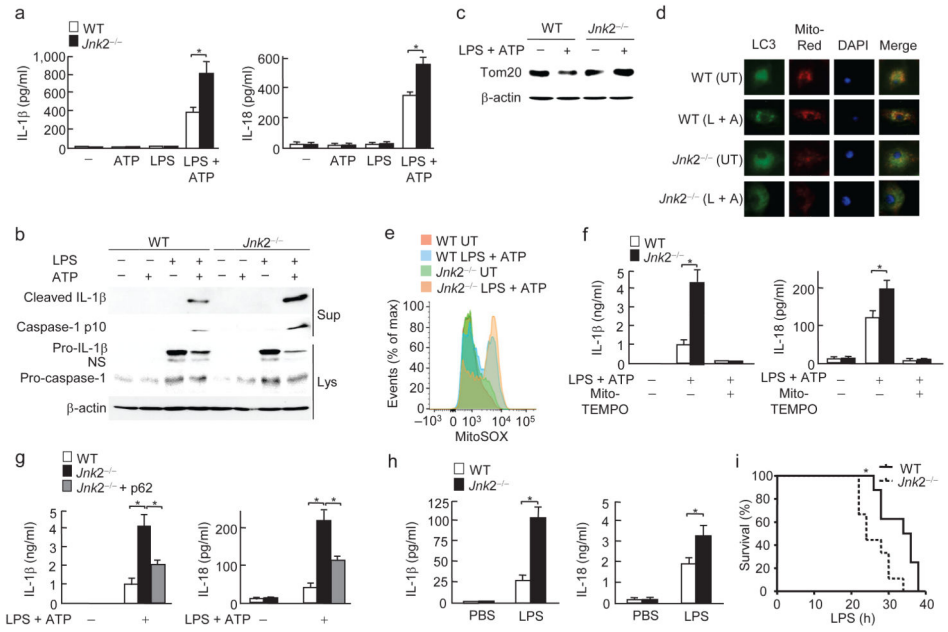

Figure 7. Loss of Jnk2 enhances inflammasome activation

(**a**) Secretion of IL-1β and IL-18 in WT and *Jnk2*$^{-/-}$ BMDMs treated with LPS and ATP. (**b**) Immunoblotting analysis of IL-1β and caspase-1 in WT and *Jnk2*$^{-/-}$ BMDMs treated with LPS and ATP. (**c**) Degradation of Tom20 in WT and *Jnk2*$^{-/-}$ BMDMs treated with LPS and ATP. (**d**) Co-localization of LC3 puncta with mitochondria in WT and *Jnk2*$^{-/-}$ BMDMs treated with LPS and ATP. (**e**) Generation of mitochondrial ROS in WT and *Jnk2*$^{-/-}$ BMDMs treated with LPS and ATP. (**f**) Secretion of IL-1β and IL-18 in WT and *Jnk2*$^{-/-}$ BMDMs pre-treated with Mito-TEMPO followed by treatment with LPS plus ATP. (**g**) Secretion of IL-1β and IL-18 in WT and *Jnk2*$^{-/-}$ BMDMs transduced with control lentiviral vector or lentiviral vector encoding Xpress-tagged p62. (**h, i**) Serum IL-1β and IL-18 levels (**h**) and survival (**i**) of WT and *Jnk2*$^{-/-}$ mice treated with intraperitoneal injection of LPS (12 mg/kg for **h** and 34 mg/kg for **i**). NS, non-specific. UT, untreated. Data are representative of five independent experiments (**a**) or three independent experiments (**b–i**); mean and s.e.m. of three mice per group with technical duplicates (**a, f, g**), or 5–6 mice per group with technical duplicates (**h**); (**i**) eight to nine mice per group; three mice per group (**b–e**). *, $P < 0.05$ by unpaired Student's *t*-test (**a, f, g, h**); $P = 0.0106$ by Log-rank Test (**i**).